Feasibility of vanadium(IV) adsorption using natural bentonite: optimization, equilibrium and kinetics

Azar Etaati, Mansooreh Soleimani*

Department of Chemical Engineering, Amirkabir University of Technology (Tehran Polytechnic), No. 350, Hafez Ave., P.O. Box: 1591634311, Tehran, Iran, emails: Soleimanim@aut.ac.ir (M. Soleimani), Azar.etaati@yahoo.com (A. Etaati)

ABSTRACT

Because of the increasing use of vanadium in different industries, including alloys and steel manufacturing, catalysts, and electrochemical coating, the presence of vanadium as toxic metal in industrial effluents has become a worldwide environmental concern. In this study, the potential of natural bentonite as an available adsorbent for vanadium(IV) ions separation was investigated. The main properties of natural bentonite were characterized using analysis such as specific surface area measurement, scanning electron microscopy, and Fourier-transform infrared spectroscopy, X-ray diffraction, and X-ray fluorescence. The influence of main adsorption parameters such as initial vanadium(IV) concentration, solution pH and adsorbent dose were also investigated. The optimization of these parameters was performed by central composite design based on response surface methodology. Based on the results, the maximum vanadium(IV) adsorption obtained at optimum conditions was 43% for initial vanadium(IV) concentration (113 mg L^{-1}), pH (2), adsorbent dosage (3.11 g L^{-1}), and contact time (180 min). The vanadium adsorption on natural bentonite was firmly confirmed by the pseudo-second-order kinetic model. The equilibrium isotherm data was fitted with the Langmuir model with significant accuracy.

Keywords: Vanadium; Natural bentonite; Optimization; Response surface methodology

1. Introduction

Vanadium is a toxic metal with different applications in rubber, photography, plants producing industrial inorganic chemicals and pigments, textile, and ceramic [1,2]. Water pollution with this heavy metal is an environmental concern. From another point of view, due to limitations in primary sources and the high economic value of vanadium, it is essential to recover vanadium from industrial effluents [3–8]. There are several treatment processes for the separation or recovery of vanadium from liquid phases, such as chemical precipitation, ion-exchange, adsorption, and membrane filtration [9–11]. Among these methods, the adsorption process is flexible, easy to operate, and less sludge disposal problems [12,13]. In recent years, many researchers have focused on finding low-cost adsorbents to decrease the cost of adsorption processes. Low-cost adsorbents include zeolite, clay, and agricultural waste, which have advantages such as low prices and natural availability [14–16]. Among these materials, clay minerals have been considered by some researchers due to their large specific surface area, layered structure, high cation exchange capacity, negative charge on their surfaces and abundance. These properties make clay minerals a suitable group of adsorbents.

Bentonite is a clay mineral with mentioned properties for clays. Therefore, it has widespread applications, including in waste disposal, lubricants, additives for cement and mortar, catalysts and catalyst supports, and water purification as adsorbents [17–21]. As mentioned above, bentonite as a low-cost and abounded adsorbent is highly regarded

---

* Corresponding author.

in industries. Due to more economic aspects, the desorption and regeneration of adsorbents have also been considered by many researchers. In commercial adsorption processes, thermal and chemical methods are used for adsorbent regenerations, but regeneration of clays has some disadvantages such as the low percentage of desorption, pollution of the adsorbent by organic solvents or inorganic chemicals, and requirement of high temperatures. The results of previous researches indicate that the desorption and regeneration process is limited due to the strong bonds of metal cations with silicate layers [22–30].

The aim of this work was to evaluate the potential of natural bentonite for vanadium adsorption from aqueous solutions. The influence of main adsorption parameters such as initial vanadium(IV) concentration, solution pH, and adsorbent dose were also investigated. Moreover, the adsorption process has been optimized using response surface methodology to determine the optimum conditions and find a model for the prediction of the amount of vanadium removal percentage vs. process parameters.

2. Materials and methods

2.1. Chemicals

Natural bentonite (NB) was provided from the Khorasan Region in Iran and used as an adsorbent. Vanadyl sulfate hydrate ($VOSO_4 \cdot 3.4H_2O$) with a purity of 97.9%, (Merck Chemical Reagents Company) and distilled water were used to prepare of vanadium stock solution. The pH of the solution was adjusted by diluted hydrochloric acid and sodium hydroxide from Merck Company.

2.2. Pretreatment of NB

In order to remove the soluble inorganic salts and any adhering materials, a pretreatment procedure was applied [19,31,32]. This step was performed by suspending NB in distilled water. This suspension liquid was stirred vigorously for 3 h on a mechanical shaker (FINEPCR, model SH30) at room temperature; then the suspension was filtrated and dried at 77°C overnight. The dried sample was ground and sieved to obtain the desired particle size (<500 μ), and stored for further usage.

2.3. Characterization of adsorbent

Since the adsorbent properties can affect the adsorption process, some of the main physical and chemical properties of the adsorbent were determined as follows:

- Chemical composition of NB was determined by using X-ray fluorescence (X unique II Rh 80KV LiF220 Gell TlAP).
- X-ray diffraction analysis was applied to identify the mineralogical compositions of NB by using an X-ray diffractometer (XRD, Philips X'PERT diffractometer, Co Kα rad).
- Surface functional groups of NB were determined by using Fourier-transform infrared spectroscopy instrument (Bruker, VERTEX 70) within the range of 400–4,000 cm⁻¹ wave number.

- Bulk density was measured by preparing a 10 mL cylinder was filled up to a specified volume with the dried adsorbent. Then the cylinder was weighed. The bulk density was then calculated by the definition [33]:

$$\text{Bulk density} = \frac{\text{Weight of dry material}(g)}{\text{Volume of packed dry material}(mL)} \quad (1)$$

- Cation exchange capacity, which is an important parameter to measure the ability of NB to remove cation metal contaminants, was measured by the Environmental Protection Agency procedure [34].
- pH_{zpc} (the pH where the net total particle charge is zero) of the NB surface was measured by adding the 0.1 g of NB to 50 mL of a 0.1 N NaCl solution. The initial pH of the solution was adjusted by HCl and NaOH. Each sample was mixed by the mechanical shaker for 24 h. After this time, the final pH of each solution was measured. If the final pH was equal to the initial pH, that pH was reported as pH_{zpc} [35].
- The specific surface area, average pore radius, and total pore volume of adsorbents were obtained by adsorption of nitrogen at 77 K (NOVA, Series-1000, Quantachrome Instruments).
- The morphologies of NB were examined before and after vanadium adsorption by a scanning electron microscope (Leo, VP 1450).

2.4. Adsorption experiments

The vanadium adsorption experiments were done in different ranges and conditions of pH, initial concentration and adsorbent dosage in a 100 mL solution. A 200 mg L⁻¹, vanadium stock solution was prepared by dissolving a certain amount of vanadyl sulfate hydrate in distilled water. The required concentration was obtained by diluting the stock solution (50–200 mg L⁻¹). The pH of the metal solution was measured and adjusted by diluted HCl and NaOH solution using a pH meter (GenWay, model). Then a certain amount of adsorbent was brought in contact with the metal solution, and shaken at 300 rpm at room temperature for a certain length of time (FINEPCR, model SH30). After the adsorption time, the adsorbent was separated by filtering using Whatman filter paper No.540, and the residual amount of vanadium in the supernatant was determined by atomic absorption spectrophotometer (AAS) (Varian AA240, wavelength of 318 nm). The amount of vanadium adsorbed was calculated from the Eq. (2):

$$\% \text{ Vanadium adsorption} = \frac{C_0 - C_f}{C_0} \times 100 \quad (2)$$

where C_0 and C_f are the initial and final vanadium concentrations (mg L⁻¹).

2.5. Design of experiment

The experimental design for optimizing of V(IV) adsorption on NB was done by applying response surface

methodology (RSM). To investigate the effect of various independent adsorption parameters such as pH (A), initial concentration (B) and, adsorbent dose (C) on V(IV) adsorption, batch experiments were conducted based on the central composite design. RSM is an excellent statistical method for the data analyzing [36,37]. The ranges and levels of coded variables based on some preliminary experiments are listed in Table 1 [38]. Based on this design, 20 experiments were conducted. The software offers a variety of polynomial models to determine the behavior of the process. The values of the correlation coefficient (R^2) were determined in order to choose the best model. The closer that R^2 is to 1, the more accurate the model. Finally, the F-value, P-value, R^2, R^2_{adj}, R^2_{pre} and, lack of fit have been analyzed for the final model.

2.6. Equilibrium studies

To study the equilibrium isotherms, the vanadium adsorption experiments were carried out with different initial conditions in the range of 25–250 mg L⁻¹. The pH of each solution and adsorbent dosage were set to their optimum values obtained by previous tests. In these tests, the samples were shaken for 24 h at 180 rpm at 25°C, 35°C, and 45°C. After 24 h, the adsorbent was separated by the filter paper, and the filtrate was used to determine of the vanadium concentration by AAS. The amount of adsorbed vanadium on the NB was calculated using Eq. (3).

$$q_e = \frac{V \times (C_0 - C_e)}{m} \qquad (3)$$

Table 1
Independence adsorption factors and their coded levels used

Independent variables	Real values of coded levels		
	−1	0	+1
A (pH)	2	6	10
B (initial concentration, mg L⁻¹)	50	125	200
C (adsorbent dosage, g L⁻¹)	1	3.5	6

where q_e (mg g⁻¹) is the amount of vanadium adsorbed on NB, V is the volume of vanadium solution (L), C_0 and C_e are initial, and equilibrium vanadium concentrations (mg L⁻¹), and m is the adsorbent mass (g).

2.7. Kinetic studies

Adsorption kinetic experiments were performed to understand the mechanism of metal adsorption. These experiments were conducted by preparing some 100 mL vanadium solutions. The pH, initial concentration, and adsorbent dosage of these solutions were adjusted to their optimal values obtained from previous tests. These solutions were stirred on a mechanical shaker at 300 rpm for different contact times in the range of 5–360 min at ambient temperature. Vanadium concentration was measured by AAS. The amount of vanadium adsorbed at time t, was obtained from Eq. (4).

$$q_t = \frac{V \times (C_0 - C_t)}{m} \qquad (4)$$

where q_t (mg g⁻¹) is the amount of vanadium adsorbed on NB after t min, V is the volume of vanadium solution (L), C_0 and C_t are initial and final vanadium concentrations at time t (mg L⁻¹), and m is adsorbent mass (g).

3. Results and discussions

3.1. Characteristics of the adsorbents

Based on X-ray fluorescence analysis, the main chemical composition of NB is reported in Table S1. It can be seen, that the percentage of calcium is higher than sodium, which means that this is a calcium type bentonite.

Fig. 1 displays the X-ray diffraction patterns of NB. It shows that smectite (S), quartz (Q), feldspar (F) and, calcite (C) are present in this sample. It can be concluded that quartz, feldspar, and calcite have created the highest impurities in the sample.

The Fourier-transform infrared (FTIR) spectra of NB was measured by a FTIR spectrometer within a range
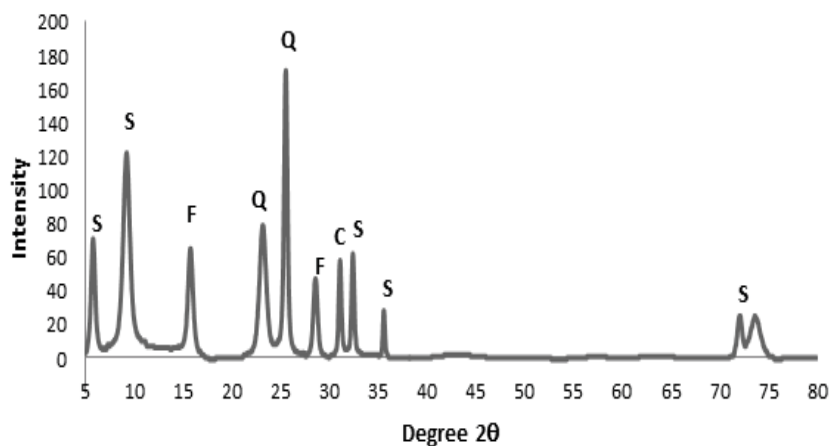
Fig. 1. X-ray diffraction patterns of natural bentonite.

of 400–4,000 cm^{-1} wave number, and it is presented in Fig. 2. A band at 466 cm^{-1} shows Si–O–Si bending vibrations. The band at 524 related to Si–O–Al bending vibration indicates that Al existed as a cation in octahedral [39]. A peak at 621 indicates the perpendicular vibration of the octahedral cations [39]. The peak at 791 indicates the presence of quartz in the sample [40]. The bands at 1,048 and 843 correspond to Si–O stretching and Al–OH–Mg bending, respectively [41]. The peaks at 3,430; 3,250 and, 1,628 cm^{-1} are related to the OH vibrational band for the water molecules that are adsorbed on clay [42,43]. Table 2 summarizes the physico-chemical properties of NB. The ion-exchange capacity for calcium bentonite in the range of 0.4–0.70 meq g^{-1}, which agrees with Table 2, is reported based on Grim [14]. The pH$_{zpc}$ value of NB is 1.60. At pH more than pH$_{zpc}$, the surface charge of NB is negative, and so there is a wide range within which the surface of NB has a good capacity for adsorption of V(IV) cations.

The values of specific surface area, total pore volume, and average pore diameter of NB were calculated and are listed in Table 2. They show that NB has a porous structure and could almost possess mesopores due to its average pore diameters, which is in the range of 20–500 Å. The scanning electron microscopy (SEM) micrographs of NB before and after vanadium adsorption at optimum adsorption conditions (pH = 2, initial vanadium concentration = 113 mg L^{-1}, and adsorbent dosage = 3.11 g L^{-1}), are displayed in Fig. 3. The results indicate that the NB has a discontinuous structure due to the absence of hydration products and the visible voids. The porosity and voids decreased after vanadium adsorption due to the presence of metal cations within the clay structure.

3.2. RSM and model fitting

A total of 20 experiments were designed for vanadium adsorption using the Design expert. The experimental conditions and adsorption percentage of each run are reported in Table 3. It can be seen that the minimum and

Table 2
Main properties of natural bentonite

Property	Value
pH$_{zpc}$	1.60
Density, (g mL^{-1})	1.04
Cation exchange capacity, (meq g^{-1})	0.65
Brunauer–Emmett–Teller surface area, (m^2 g^{-1})	53.97
Total pore volume, ×10^{-3}, (cm^3 g^{-1})	84.76
Average pore diameter, (Å)	31.44
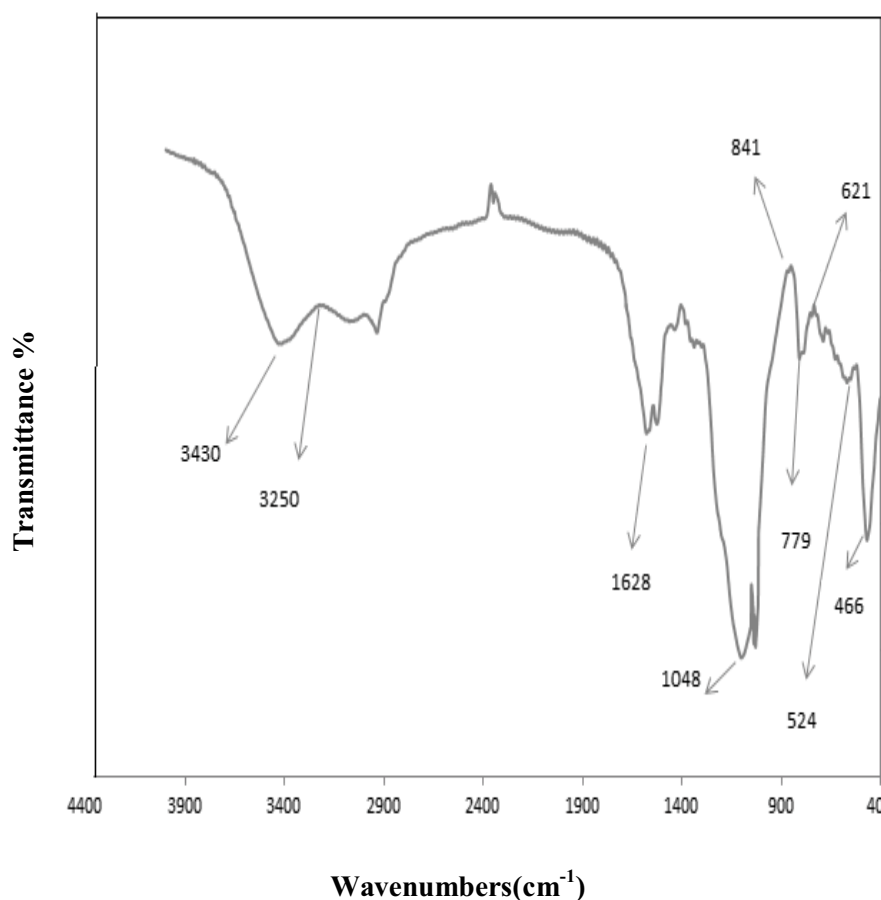
Fig. 2. FTIR spectra of natural bentonite.

(a)

(b)

(c)

(d)
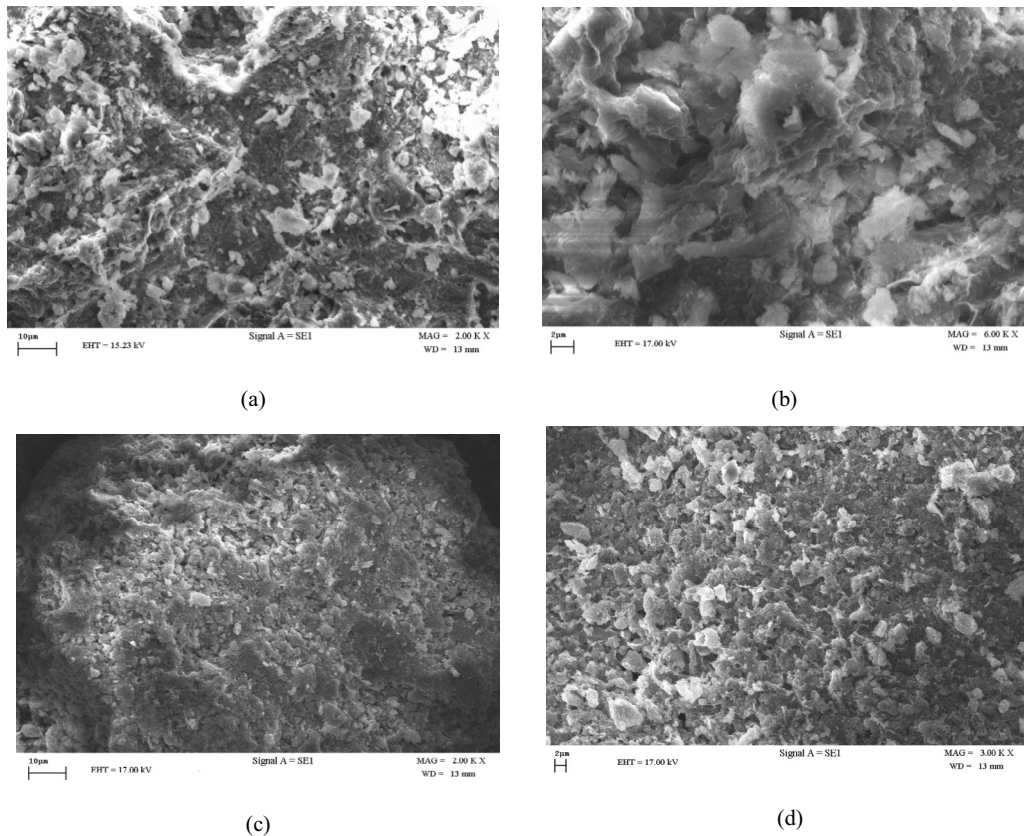
Fig. 3. SEM photographs (a) 2,500×, (b)10,000× of natural bentonite and (c) 2,500×, (d) 10,000× after vanadium adsorption at optimum conditions (pH = 2, initial vanadium concentration = 113 mg L^{-1} and adsorbent dosage = 3.11 g L^{-1}).

Table 3
The corresponding experimental conditions and obtained responses

No.	pH	C_0 (mg L^{-1})	M (g L^{-1})	% adsorption
1	2	200	6.00	41.24
2	2	200	1.00	39.86
3	10	200	1.00	32.00
4	10	200	6.00	32.17
5	6	200	3.50	31.62
6	2	50	6.00	42.19
7	2	50	1.00	37.55
8	6	50	3.50	21.55
9	10	50	1.00	22.46
10	10	50	6.00	21.34
11	6	125	3.50	31.78
12	6	125	6.00	32.69
13	6	125	3.50	32.42
14	6	125	1.00	30.72
15	6	125	3.50	27.78
16	6	125	3.50	32.10
17	6	125	3.50	29.78
18	6	125	3.50	30.10
19	2	125	3.50	39.99
20	10	125	3.50	32.33

maximum adsorption percentages are about 21% and 42%, respectively.

Analysis of variance (ANOVA) was performed to verify the accuracy and efficiency of the model [36,44], and the results for vanadium adsorption are shown in Table 4. It can be seen that the proposed model is adequate for an *F*-value of 25.1. The small amount of *P*-value (<0.0001) also confirms the same result. All the parameters in ANOVA with *P*-values higher than 0.1 have no significant impact on the model, and have been deleted [36,44]. However, two parameters *C*, and *AC* that ordinarily represent the adsorbent dosage, and interaction between pH and the adsorbent dosage, have not been removed. In fact, it was observed that with these two parameters in the final model, the adequacy of the model was improved. The adequate precision ratio of the model was 17.54, which represents an adequate signal for the model (adequate precision >4) [45,46]. The final model is shown in Eq. (5):

$$\% \text{ Adsorption} = 30.75 - 6.05A + 3.18B + 0.70C$$
$$+ 2.37AB - 0.87AC + 6.13A^2 - 3.45B^2 \quad (5)$$

It could be concluded that the above equation is a quadratic model. The value of the coefficient of determination for the model was $R^2 = 0.9359$, which indicates that the quadratic model has a high degree of accuracy and the ability of model to predict changes in data is at least 93.59%.

Also, the amounts of R^2_{adj} and R^2_{pre} were 0.8984 and 0.7942, respectively. These values demonstrate that the model fits the experimental data quite well. The value of 1.28 for the *F*-value of the lack of fit indicates that the systematic variation will not impact on the model. These results suggest that the proposed model has high accuracy and good ability to find the optimum conditions for maximum adsorption.

Fig. S1 shows the plot of predicted vs. actual values. According to this figure, the data points are located on a straight line which indicates a good relationship between the experimental and predicted values.

The 3D surface response is depicted in Fig. 4. To draw this chart, one of the variables was fixed in optimal value, and the variations of two other parameters were

Table 4
Analysis of variance (ANOVA) for the quadratic model

Source	Sum of squares	Degree of freedom	Mean square	*F*-value	Prob. > *F*
Model	643.9500	7	91.9900	25.0100	<0.0001
A-pH	366.2700	1	366.2700	99.5900	<0.0001
B-C_0	101.1200	1	101.1200	27.4900	0.0002
C-*M*	4.9700	1	4.9700	1.3500	0.2627
AB	45.1300	1	45.1300	12.2700	0.0044
AC	6.0900	1	6.0900	1.6600	0.2224
A^2	120.1200	1	120.1200	32.6600	<0.0001
B^2	38.1600	1	38.1600	10.3700	0.0037
Residual	44.1400	12	3.8600	–	–
Lack of fit	28.3300	7	4.0500	1.2800	0.4064
Pure error	5.8100	5	3.1600	–	–

(a)

(b)

(c)
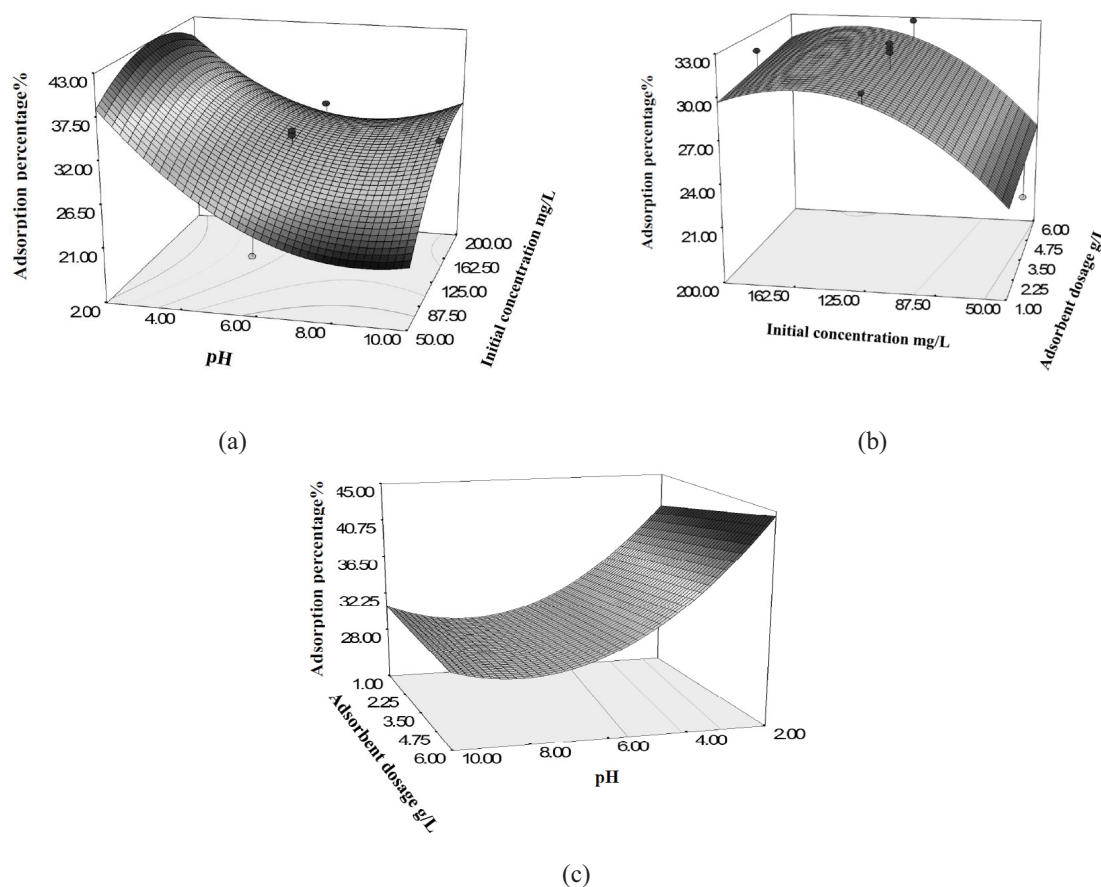
Fig. 4. 3D surface response for vanadium adsorption with natural bentonite vs. (a) pH and initial concentration, at adsorbent dosage = 3.11 g L^{-1}, (b) adsorbent dosage and initial concentration, at pH = 2, and (c) adsorbent dosage and pH at initial concentration = 113 mg L^{-1}.

investigated. It can be seen from Fig. S2a and b that the vanadium adsorption initially increased with increasing the vanadium concentration, and then began to decrease. This phenomenon is due to the increased driving force to achieve maximum value, which saturated the adsorbent and caused the gradual loss of its ability to adsorb cations from the aqueous solution. According to Fig. 4c, vanadium adsorption began to increase by increasing the adsorbent dosage, confirming similar results that have been reported in the literature [47,48].

3.3. Numerical optimization

The main objective of this paper is to determine the optimal conditions for maximum vanadium adsorption. Based on the results, at pH = 2, initial concentration of 113 mg L^{-1} and adsorbent dosage of 3.11 g L^{-1}, the maximum vanadium adsorption percentage and maximum adsorption capacity were achieved at about 43% and 15.62 mg g^{-1}, respectively. By conducting experiments with the optimal conditions, a good agreement between the model and experiment data was obtained (relative error of about 7%).

The maximum adsorption capacity of other adsorbents for vanadium is presented in Table 5. As can be seen, the adsorption capacity for NB is comparable to other adsorbents.

3.4. Adsorption isotherms

The study of adsorption isotherms is helpful to understand the mechanism between the adsorbent and adsorbate. The isotherms of Langmuir, Freundlich and Temkin were the main isotherms applied in this project. The linear form of Langmuir isotherm is given by Eq. (6):

$$\frac{C_e}{q_e} = \frac{1}{k_l} + \frac{a_1}{k_l} C_e \tag{6}$$

where q_e is the amount of vanadium adsorbed on NB (mg g^{-1}), C_e is the equilibrium concentration (mg L^{-1}), a_1 (L mg^{-1}),

and k_l (L g^{-1}) are Langmuir constants [49]. R_l is defined by Eq. (7) as a dimensionless equilibrium parameter.

$$R_l = \frac{1}{1 + a_1 C_0} \tag{7}$$

The desired level of adsorption isotherm can be realized by the R_l parameter. $R_l > 1$ shows the undesirable isotherm, $R_l = 1$ shows the linear form and $R_l < 1$ shows a favorable isotherm [38].

Freundlich isotherm is an empirical equation that is used to describe reversible, non-ideal, and multi-layered adsorption. An adsorbent that follows the Freundlich model has a heterogeneous surface and areas with a different potential for adsorption. The linear form of the Freundlich model is shown by Eq. (8):

$$\log q_e = \frac{1}{n} \log C_e + \log k_f \tag{8}$$

where k_f and $1/n$ are the Freundlich constants that are related to the adsorption capacity of adsorbent (mg g^{-1} L$^{1/n}$ mg$^{-1/n}$) and adsorption intensity, respectively [50]. The amount of $1/n$ represents the amount of heterogeneous surface of the adsorbent, and the closer it is to zero, the more heterogeneous the adsorbent surface will be.

In the Temkin model, it is assumed that the heat adsorption of all molecules in the layer will decrease linearly when the adsorption layer increases. The isotherm equation is given:

$$q_e = \beta \ln k_t + \beta \ln C_e \tag{9}$$

where k_t (L mg^{-1}) represents the maximum binding energy, and β (J mol^{-1}) is dependent on the heat of adsorption [51]. The values of all parameters are reported in Table 6.

In Fig. S2, the equilibrium adsorption data that was predicted by the models are plotted vs. the equilibrium

Table 5
Vanadium adsorption capacity of different adsorbents

Adsorbent	pH	Initial concentration (mg L^{-1})	Adsorbent dosage (g L^{-1})	Adsorption capacity (mg g^{-1})	References
Aluminum-pillared bentonite	2.0–8.0	5–50	4.0	2.48	(Manohar, Noeline et al. 2005)
Crosslinked chitosan	4.0–4.5	–	0.6	6.27	(Qian, Wang et al. 2004)
Commercial activated carbon	4.5	25.0–200.0	1.0	37.78	(Sharififard and Soleimani, 2015)
Metal (hydr)oxide: E 33[a]	2.0–11.0	1–250	1.0–5.0	25.00	(Naeem, Westerhoff et al. 2007)
Fe(III)/Cr(III) hydroxide	4.0–10.0	10–40	10.0	11.43	(Prathap and Namasivayam, 2010)
His-multi-walled carbon nanotubes (MWCNTs)	5.5	1–8	0.8	4.85	(Liu, Li et al. 2012)
Natural bentonite	2.0–10.0	50–200	1.0–6.0	15.62	This work

[a]Bayoxide® E 33 with iron oxide media.

Table 6
Isotherm model parameters for vanadium adsorption on natural bentonite

Isotherm models	Parameters	25°C	35°C	45°C
Langmuir	q_m (mg g^{-1})	30.3951	58.8235	29.2397
	a_1 (L mg^{-1})	0.0102	0.0042	0.0100
	k_l (L g^{-1})	0.3103	0.2501	0.2937
	R_l	0.7968–0.2817	0.9050–0.4878	0.8–0.2857
	R^2	0.9669	0.9786	0.9822
Freundlich	N	1.7790	1.3764	1.5696
	k_f	1.0318	0.5438	0.7389
	R^2	0.9126	0.9720	0.9578
Temkin	β (J mol^{-1})	4.1648	7.3565	6.2260
	k_t (L mg^{-1})	0.0053	0.0048	0.0061
	R^2	0.8013	0.9744	0.8851

concentration at different temperatures. As can be seen from these figures, the Langmuir isotherm is the best model to fit the experimental data. This result was confirmed by the comparison of R^2 of all models. As shown in Table 6, the amount of R^2 for Langmuir isotherm is higher than other isotherm models. This indicates that the adsorption took place on a single layer and in all parts of the homogeneous surface. The value of R_l was calculated for all temperatures in the vanadium adsorption process, and they show that adsorption is a favorable process for vanadium removal.

3.5. Adsorption kinetics

The main kinetic models, including pseudo-first-order, pseudo-second-order, and intraparticle diffusion were investigated to understand the mechanisms of adsorption and the controlling rate step for vanadium adsorption.

The pseudo-first-order model is a simple model that is widely used for adsorption from the liquid phase and shown in Eq. (10).

$$\log(q_e - q_t) = \log q_e - \frac{k_1 t}{2.303} \tag{10}$$

where q_t and q_e are the amount of vanadium adsorbed per unit of adsorbent (mg g^{-1}) at equilibrium and time t (mg g^{-1}), respectively. k_1 is the pseudo-first-order rate constant (min^{-1}), and t is the contact time (min) [52].

The pseudo-second-order model is presented by the Eq. (11):

$$\frac{t}{q_t} = \frac{1}{k_2 q_e^2} + \frac{t}{q_e} \tag{11}$$

where k_2 (g mg^{-1} min^{-1}) is the equilibrium rate constant of the pseudo-second-order model [53].

Weber–Morris indicated that in many adsorption processes, the amount of adsorbed was proportional to $t^{0.5}$ by the Eq. (12):

$$q_t = k_3 t^{0.5} + C \tag{12}$$

Table 7
Kinetic model parameters for vanadium adsorption

Experimental	q_e (mg g^{-1})	14.2604
First-order kinetic model	k_1 (min^{-1})	0.0292
	q_e (mg g^{-1})	0.8509
	R^2	0.9551
Second-order kinetic model	k_2	0.1424
	q_e (mg g^{-1})	14.2857
	R^2	1
Intraparticle diffusion	k_3	0.0232
	C	13.891
	R^2	0.8720

where k_3 (mg g^{-1} min$^{-0.5}$) is the intraparticle diffusion rate constant, and C (mg g^{-1}) is the intercept that indicates the role of the boundary layer in controlling the mass transfer mechanism. A plot of $q_t \sim t^{0.5}$ for this should be a straight line. However, if the plot does not go through the origin, the intraparticle diffusion could not be the only mechanism involved [54].

Fig. S3 presents the linear plots of kinetic models. The calculated kinetic parameters and their R^2 values are reported in Table 7. The results demonstrate that the pseudo-second-order kinetic model is the best model compared to other models. The high R^2 value for this model confirms this conclusion. Also, the results show that the vanadium adsorption was controlled by chemisorption involving valence forces through sharing or exchange of electrons. Therefore, the main mechanism is an ion exchange process. The metals located in the exchangeable sites of natural bentonite are replaced with vanadium cations present in the aqueous solution. Another mechanism that may have occurred is the formation of vanadium hydroxide species which may result from either participation in the adsorption or precipitation onto the bentonite.

4. Conclusions

Bentonite is natural clay with a layered structure, high surface area, high cation exchange capacity, and negative

charges on its surface. The main objective of this paper was to evaluate the potential of natural bentonite as a low-cost adsorbent for vanadium separation from aqueous solutions. The analysis of SEM indicated that NB has a discontinuous structure that becomes more coherent after vanadium adsorption. The FTIR analysis determined the main functional groups such as Al–OH–Mg on the NB surface. The response surface methodology was used to find a highly significant and very low probability value model for the vanadium adsorption process, and determine the optimum process conditions. The adsorption efficiency of V(IV) at the optimum experimental condition of initial vanadium(IV) concentration (113 mg L^{-1}), pH (2), adsorbent dose (3.11 g L^{-1}), and contact time (180 min) was 43%. The high values of R^2 for predicted vs. actual plot show that this model is in good agreement with the experimental data. The analysis of the equilibrium data showed that the Langmuir model was the best model for describing the equilibrium adsorption of vanadium on bentonite. The kinetic studies showed that the pseudo-second-order model was quite valid for the adsorption process and indicates a multi-step diffusion for this process, such as chemisorption involving valence forces through sharing or exchange of electrons. The main advantages of bentonite as an adsorbent are its cheapness and abundance. For commercial use, further studies on desorption and regeneration of adsorbent should be performed.

Symbols

C_0	—	Initial vanadium concentration, mg L^{-1}
C_f	—	Final vanadium concentration, mg L^{-1}
q_e	—	Amount of vanadium adsorbed per unit weight of the adsorbent at equilibrium, mg g^{-1}
V	—	Volume of the solution, L
C_e	—	Equilibrium vanadium concentration, mg L^{-1}
m	—	Mass of dry adsorbent, g
q_t	—	Amount of vanadium adsorbed per unit weight of the adsorbent at time t, mg g^{-1}
C_t	—	Vanadium concentration at the time t, mg L^{-1}
k_l	—	Langmuir isotherm constant, L g^{-1}
a_1	—	Langmuir isotherm constant, L mg^{-1}
R_l	—	Dimensionless equilibrium parameter
n	—	Freundlich isotherm constant, heterogeneity factor
k_f	—	Freundlich isotherm constant, adsorption capacity, (mg g^{-1} L$^{1/n}$ mg$^{-1/n}$)
β	—	Temkin isotherm constant, that is related to the heat of adsorption, J mol^{-1}
k_t	—	Equilibrium binding constant that is related to the maximum binding energy, L mg^{-1}
k_1	—	Rate constant of pseudo-first-order kinetic model, min^{-1}
t	—	Contact time, min
k_2	—	Rate constant of pseudo-second-order kinetic model, g mg^{-1} min^{-1}
k_3	—	Rate constant of intraparticle diffusion kinetic model, mg g^{-1} min$^{-0.5}$
C	—	Intercept of intraparticle diffusion kinetic model, mg g^{-1}

References

[1] D.C. Crans, J.J. Smee, E. Gaidamauskas, L. Yang, The chemistry and biochemistry of vanadium and the biological activities exerted by vanadium compounds, Chem. Rev., 104 (2004) 849–902.

[2] D.M. Manohar, B.F. Noeline, T.S. Anirudhan, Removal of vanadium(IV) from aqueous solutions by adsorption process with aluminum-pillared bentonite, Ind. Eng. Chem. Res., 44 (2005) 6676–6684.

[3] M. Poorbaba, M. Soleimani, Single and competitive adsorption of V-EDTA and Ni-EDTA complexes onto activated carbon: response surface optimization, kinetic, equilibrium, and thermodynamic studies, Desal. Water Treat., 212 (2021) 185–203.

[4] R. Moskalyk, A. Alfantazi, Processing of vanadium: a review, Miner. Eng., 16 (2003) 793–805.

[5] T. Anirudhan, P. Radhakrishnan, Adsorptive performance of an amine-functionalized poly(hydroxyethylmethacrylate)-grafted tamarind fruit shell for vanadium(V) removal from aqueous solutions, Chem. Eng. J., 165 (2010) 142–150.

[6] N. Kocak, M. Sahin, I.H. Gubbuk, Synthesized of sporopollenin-immobilized Schiff bases and their vanadium(IV) sorption studies, J. Inorg. Organomet. Polym. Mater., 22 (2012) 852–859.

[7] H. Sharififard, M. Soleimani, Performance comparison of activated carbon and ferric oxide-hydroxide–activated carbon nanocomposite as vanadium(V) ion adsorbents, RSC Adv., 5 (2015) 80650–80660.

[8] M. Poorbaba, M. Soleimani, Recovery of vanadium-EDTA complex from extraction leachate of vanadium secondary resources: optimization and experimental investigation, Desal. Water Treat., 101 (2018) 268–282.

[9] A. Padilla-Rodríguez, J.A. Hernández-Viezcas, J.R. Peralta-Videa, J.L. Gardea-Torresdey, O. Perales-Pérez, F.R. Román-Velázquez, Synthesis of protonated chitosan flakes for the removal of vanadium(III, IV and V) oxyanions from aqueous solutions, Microchem. J., 118 (2015) 1–11.

[10] A. Bhatnagar, A. Kumar Minocha, D. Pudasainee, H. Chung, S. Kim, H. Kim, G. Lee, B. Min, B. Jeon, Vanadium removal from water by waste metal sludge and cement immobilization, Chem. Eng. J., 144 (2008) 197–204.

[11] J. Hu, X. Wang, L. Xiao, S. Song, B. Zhang, Removal of vanadium from molybdate solution by ion exchange, Hydrometallurgy, 95 (2009) 203–206.

[12] Z.-r. Liu, S. Zhou, Adsorption of copper and nickel on Na-bentonite, Process Saf. Environ. Prot., 88 (2010) 62–66.

[13] H. Sharififard, M. Soleimani, F. Zokaee Ashtiani, Application of nanoscale iron oxide-hydroxide-impregnated activated carbon (Fe-AC) as an adsorbent for vanadium recovery from aqueous solutions, Desal. Water Treat., 57 (2016) 15714–15723.

[14] R.E. Grim, Applied Clay Mineralogy, McGraw-Hill, New York, 1962.

[15] S. Babel, T.A. Kurniawan, Low-cost adsorbents for heavy metals uptake from contaminated water: a review, J. Hazard. Mater., 97 (2003) 219–243.

[16] Y. Min, Y. Zhou, M. Zhang, H. Qiao, Q. Huang, T. Ma, Removal of ionic liquid by engineered bentonite from aqueous solution, J. Taiwan Inst. Chem. Eng., 53 (2015) 153–159.

[17] M. Mercurio, B. Sarkar, A. Langella, Modified Clay and Zeolite Nanocomposite Materials Environmental and Pharmaceutical Applications, Elsevier, 2019, pp.113–127

[18] G. Brauer, Handbook of Preparative Inorganic Chemistry V2, Academic Press Inc., London, 1963.

[19] S. Mirmohamadsadeghi, T. Kaghazchi, M. Soleimani, N. Asasian, An efficient method for clay modification and its application for phenol removal from wastewater, Appl. Clay Sci., 59 (2012) 8–12.

[20] F. Bergaya, G. Lagaly, Handbook of Clay Science, Elsevier Newnes, 2013.

[21] A. Rahmani, G.R. Karimi, M. Hosseini, Removal/separation of Co(II) ion from environmental sample solutions by $MnFe_2O_4$/bentonite nanocomposite as a magnetic nanomaterial, Desal. Water Treat., 89 (2017) 250–257.

[22] D. Xu, X. Zhou, X. Wang, Adsorption and desorption of Ni^{2+} on Na-montmorillonite: effect of pH, ionic strength, fulvic acid, humic acid and addition sequences, Appl. Clay Sci., 39 (2008) 133–141.

[23] M. Al-Qunaibit, W. Mekhemer, A. Zaghloul, The adsorption of Cu(II) ions on bentonite—a kinetic study, J. Colloid Interface Sci., 283 (2005) 316–321.

[24] N. Cavallaro, M. McBride, Copper and cadmium adsorption characteristics of selected acid and calcareous soils, Soil Sci. Soc. Am. J., 42 (1978) 550–556.

[25] S. Mishra, Adsorption–desorption of heavy metal ions, Curr. Sci., 2014 601–612.

[26] O. Korkut, E. Sayan, O. Lacin, B. Bayrak, Investigation of adsorption and ultrasound assisted desorption of lead(II) and copper(II) on local bentonite: a modelling study, Desalination, 259 (2010) 243–248.

[27] T. Undabeytia, S. Nir, G. Rytwo, C. Serban, E. Morillo, C. Maqueda, Modeling adsorption–desorption processes of cu on edge and planar sites of montmorillonite, Environ. Sci. Technol., 36 (2002) 2677–2683.

[28] X. Peng, Z. Luan, H. Zhang, Montmorillonite–Cu(II)/Fe(III) oxides magnetic material as adsorbent for removal of humic acid and its thermal regeneration, Chemosphere, 63 (2006) 300–306.

[29] R. Antonelli, G.R.P. Malpass, M.G.C. da Silva, M.G.A. Vieira, Adsorption of ciprofloxacin onto thermally modified bentonite clay: experimental design, characterization, and adsorbent regeneration, J. Environ. Chem. Eng., 8 (2020) 104553, doi: 10.1016/j.jece.2020.104553.

[30] F. Banat, B. Al-Bashir, S. Al-Asheh, O. Hayajneh, Adsorption of phenol by bentonite, Environ. Pollut., 107 (2000) 391–398.

[31] A.A. Moosa, A.M. Ridha, I.N. Abdullha, Chromium ions removal from wastewater using activated Iraqi Bentonite, Int. J. Innov. Res. Sci. Eng. Technol., 4 (2015) 15–25.

[32] E. Eren, B. Afsin, An investigation of Cu(II) adsorption by raw and acid-activated bentonite: a combined potentiometric, thermodynamic, XRD, IR, DTA study, J. Hazard. Mater., 151 (2008) 682–691.

[33] F.D. Snell, C.L. Hilton, L.S. Ettre, Encyclopedia of Industrial Chemical Analysis, Interscience Publishers, New York, 1966.

[34] E. Taiwan, Cation Exchange Capacity of Soils, Method NIEA. S., 202 (1994) 60A.

[35] S.A. Dastgheib, D.A. Rockstraw, A model for the adsorption of single metal ion solutes in aqueous solution onto activated carbon produced from pecan shells, Carbon, 40 (2002) 1843–1851.

[36] D.C. Montgomery, Design and Analysis of Experiments, John Wiley & Sons Inc., New York, NY, 2012.

[37] M.J. Bashir, H.A. Aziz, M.S. Yusoff, M.N. Adlan, Application of response surface methodology (RSM) for optimization of ammoniacal nitrogen removal from semi-aerobic landfill

[38] A. Etaati, M. Soleimani, Optimizing of vanadium adsorption onto natural bentonite using response surface methodology, Int. J. Chem. Environ. Eng., 6 (2015) 357–361.

[39] J. Madejová, J. Bujdák, M. Janek, P. Komadel, Comparative FTIR study of structural modifications during acid treatment of dioctahedral smectites and hectorite, Spectrochim. Acta, Part A, 54 (1998) 1397–1406.

[40] S. Yang, D. Zhao, H. Zhang, S. Lu, L. Chen, X. Yu, Impact of environmental conditions on the sorption behavior of Pb(II) in Na-bentonite suspensions, J. Hazard. Mater., 183 (2010) 632–640.

[41] A.S. Özcan, A. Özcan, Adsorption of acid dyes from aqueous solutions onto acid-activated bentonite, J. Colloid Interface Sci., 276 (2004) 39–46.

[42] F. Ayari, E. Srasra, M. Trabelsi-Ayadi, Characterization of bentonitic clays and their use as adsorbent, Desalination, 185 (2005) 391–397.

[43] L. Yaming, B. Mingliang, W. Zhipeng, L. Run, S. Keliang, W. Wangsuo, Organic modification of bentonite and its application for perrhenate (an analogue of pertechnetate) removal from aqueous solution, J. Taiwan Inst. Chem. Eng., 62 (2016) 104–111.

[44] N. Mehrabi, M. Soleimani, M.M. Yeganeh, H. Sharififard, Parameter optimization for nitrate removal from water using activated carbon and composite of activated carbon and Fe_2O_3 nanoparticles, RSC Adv., 5 (2015) 51470–51482.

[45] M.R. Hormozi-Nezhad, H. Robatjazi, M. Jalali-Heravi, Thorough tuning of the aspect ratio of gold nanorods using response surface methodology, Anal. Chim. Acta, 779 (2013) 14–21.

[46] M. Mourabet, A. El Rhilassi, H. El Boujaady, M. Bennani-Ziatni, A. Taitai, Use of response surface methodology for optimization of fluoride adsorption in an aqueous solution by Brushite, Arabian J. Chem., 10 (2017) S3292-S3302.

[47] P. Sudamalla, P. Saravanan, M. Matheswaran, Optimization of operating parameters using response surface methodology for adsorption of crystal violet by activated carbon prepared from mango kernel, Sustainable Environ. Res., 22 (2012) 1–7.

[48] B. Das, N.K. Mondal, P. Roy, S. Chattoraj, Application of response surface methodology for hexavalent chromium adsorption onto alluvial soil of Indian origin, Int. J. Environ. Pollut., 2 (2013) 72–87.

[49] V. Vimonses, S. Lei, B. Jin, C.W. Chow, C. Saint, Kinetic study and equilibrium isotherm analysis of Congo red adsorption by clay materials, Chem. Eng. J., 148 (2009) 354–364.

[50] M.A. Tabatabai, D.L. Sparks, L. Al-Amoodi, W. Dick, Chemical Processes in Soils, Soil Science Society of America Inc., 2005.

[51] K.G. Akpomie, F.A. Dawodu, Potential of a low-cost bentonite for heavy metal abstraction from binary component system, J. Assoc. Arab. Univ. Basic Appl. Sci., 4 (2015) 1–13.

[52] H. Qiu, L. Lv, B.-c. Pan, Q.-j. Zhang, W.-m. Zhang, Q.-x. Zhang, Critical review in adsorption kinetic models, J. Zhejiang Univ. Sci., A, 10 (2009) 716–724.

[53] N. Mehrabi, M. Soleimani, H. Sharififard, M. Madadi Yeganeh, Optimization of phosphate removal from drinking water with activated carbon using response surface methodology (RSM), Desal. Water Treat., 57 (2016) 15613–15618.

[54] B.H. Hameed, A.A. Ahmad, Batch adsorption of methylene blue from aqueous solution by garlic peel, an agricultural waste biomass, J. Hazard. Mater., 164 (2009) 870–875.

Supplementary information

Table S1
The chemical composition of natural bentonite

Chemical compound	(%) wt.
SiO_2	66.66
Al_2O_3	11.11
Fe_2O_3	4.38
MgO	2.76
CaO	2.31
Na_2O	1.05
K_2O	0.64
TiO_2	0.44
SO_3	0.23
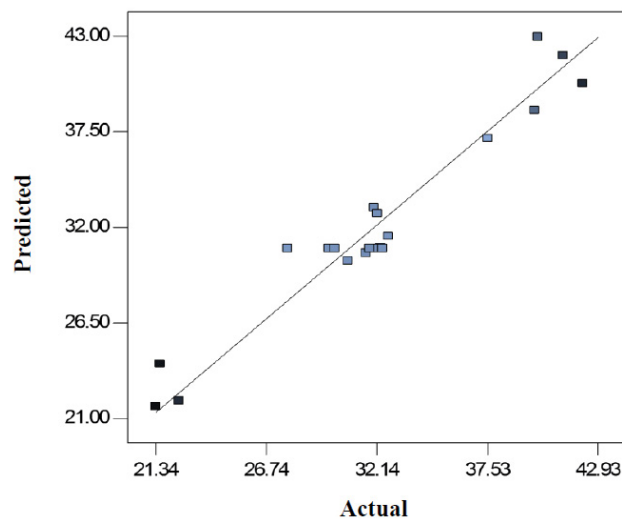
Fig. S1. Predicted vs. actual values plot for vanadium adsorption.
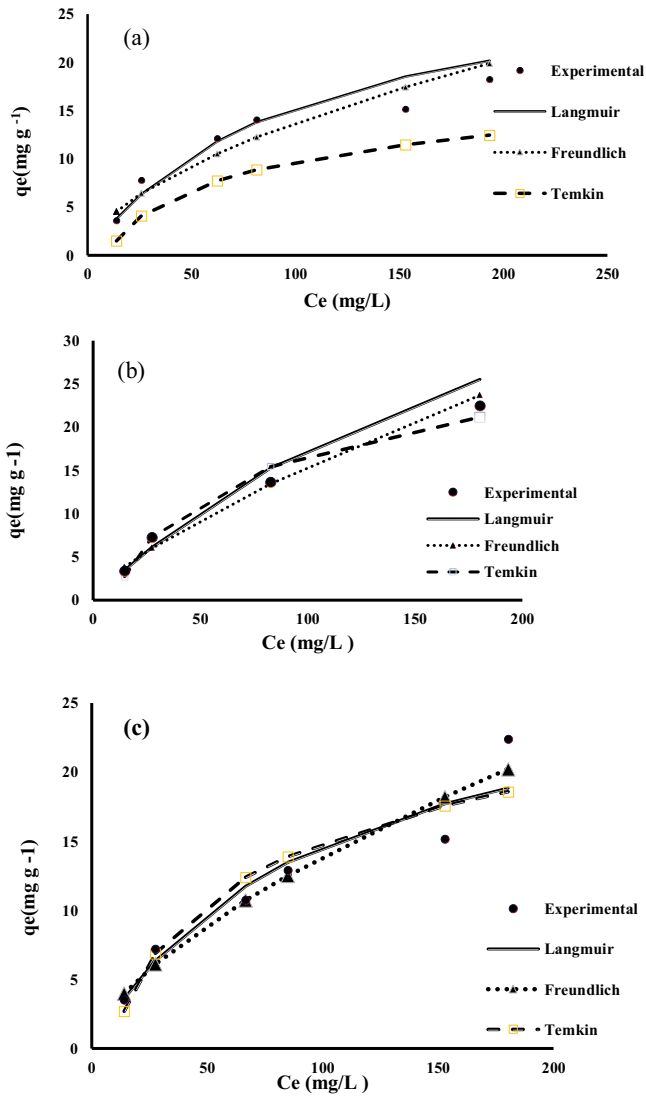
Fig. S2. Isotherm plots for vanadium adsorption on natural bentonite at (a) 25°C, (b) 35°C, and (c) 45°C.
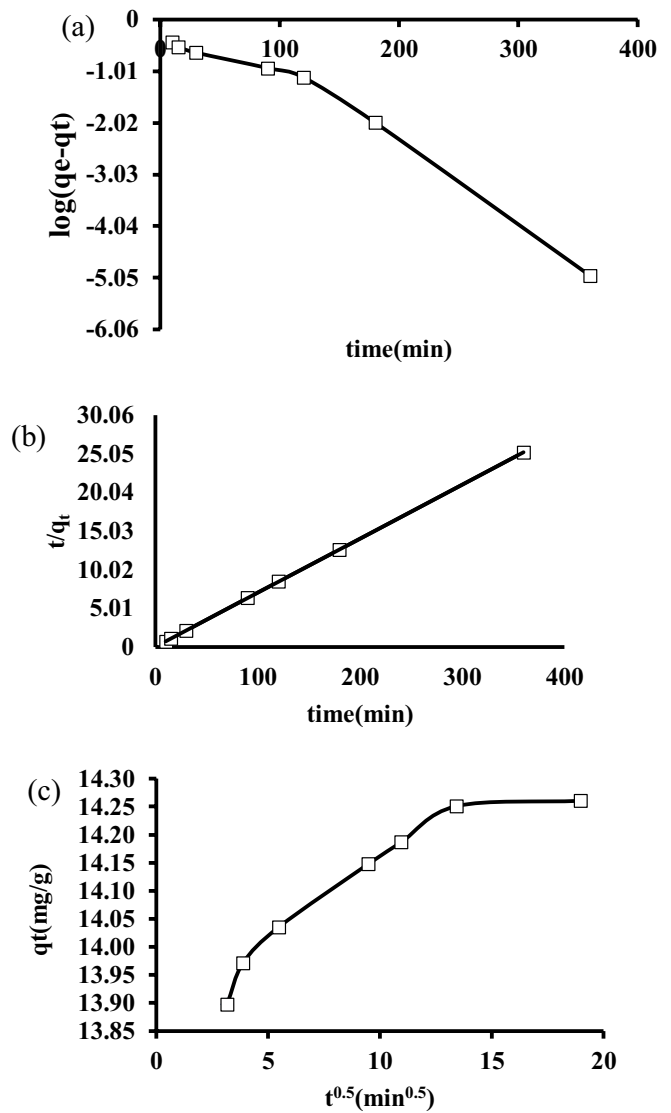
Fig. S3. (a) Pseudo-first-order model, (b) pseudo-second-order model, and (c) intraparticle diffusion model at optimum adsorption condition (pH = 2, initial vanadium concentration = 113 mg L^{-1} and adsorbent dosage = 3.11 g L^{-1}).